

RESEARCH ARTICLE

# A new synthetic matrix metalloproteinase inhibitor reduces human mesenchymal stem cell adipogenesis

Dale B. Bosco<sup>1<sup>aa</sup></sup>, Mark D. Roycik<sup>2<sup>ab</sup></sup>, Yonghao Jin<sup>2<sup>ac</sup></sup>, Martin A. Schwartz<sup>2</sup>, Ty J. Lively<sup>2</sup>, Diego A. R. Zorio<sup>2<sup>aa</sup></sup>, Qing-Xiang Amy Sang<sup>1,2\*</sup>

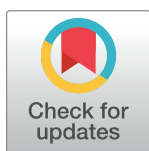
**1** Institute of Molecular Biophysics, Florida State University, Tallahassee, Florida, United States of America, **2** Department of Chemistry & Biochemistry, Florida State University, Tallahassee, Florida, United States of America

<sup>aa</sup> Current address: Department of Biomedical Sciences, College of Medicine, Florida State University, Tallahassee, Florida, United States of America

<sup>ab</sup> Current address: Department of Biology and Marine Science, Jacksonville University, Jacksonville, Florida, United States of America

<sup>ac</sup> Current address: College of Pharmacy and Pharmaceutical Science, Florida A&M University, Tallahassee, Florida, United States of America

\* [qxsang@chem.fsu.edu](mailto:qxsang@chem.fsu.edu)



**OPEN ACCESS**

**Citation:** Bosco DB, Roycik MD, Jin Y, Schwartz MA, Lively TJ, Zorio DAR, et al. (2017) A new synthetic matrix metalloproteinase inhibitor reduces human mesenchymal stem cell adipogenesis. *PLoS ONE* 12(2): e0172925. doi:10.1371/journal.pone.0172925

**Editor:** Ming Tan, University of South Alabama, UNITED STATES

**Received:** December 9, 2016

**Accepted:** February 10, 2017

**Published:** February 24, 2017

**Copyright:** © 2017 Bosco et al. This is an open access article distributed under the terms of the [Creative Commons Attribution License](https://creativecommons.org/licenses/by/4.0/), which permits unrestricted use, distribution, and reproduction in any medium, provided the original author and source are credited.

**Data Availability Statement:** All relevant data are within the paper.

**Funding:** This work was supported in part by grants from the Florida Department of Health James and Esther King Biomedical Research Program (Grant 1KF04), Florida State University, and anonymous donors for an Endowed Chair Professorship in Cancer Research (to QXAS), and by the Molecular Design and Synthesis (MDS) Foundation (to MAS). The funders had no role in

## Abstract

Development of adipose tissue requires the differentiation of less specialized cells, such as human mesenchymal stem cells (hMSCs), into adipocytes. Since matrix metalloproteinases (MMPs) play critical roles in the cell differentiation process, we conducted investigations to determine if a novel mercaptosulfonamide-based MMP inhibitor (MMPI), YHJ-7-52, could affect hMSC adipogenic differentiation and lipid accumulation. Enzyme inhibition assays, adipogenic differentiation experiments, and quantitative PCR methods were employed to characterize this inhibitor and determine its effect upon adipogenesis. YHJ-7-52 reduced lipid accumulation in differentiated cells by comparable amounts as a potent hydroxamate MMPI, GM6001. However, YHJ-7-82, a non-inhibitory structural analog of YHJ-7-52, in which the zinc-binding thiol group is replaced by a hydroxyl group, had no effect on adipogenesis. The two MMPis (YHJ-7-52 and GM6001) were also as effective in reducing lipid accumulation in differentiated cells as T0070907, an antagonist of peroxisome-proliferator activated receptor gamma (PPAR-gamma), at a similar concentration. PPAR-gamma is a typical adipogenic marker and a key regulatory protein for the transition of preadipocyte to adipocyte. Moreover, MMP inhibition was able to suppress lipid accumulation in cells co-treated with Troglitazone, a PPAR-gamma agonist. Our results indicate that MMP inhibitors may be used as molecular tools for adipogenesis and obesity treatment research.

## Introduction

Obesity is an epidemic affecting one-third of Americans [1, 2]. This disorder is a major risk factor for numerous conditions, including cardiovascular disease, stroke, diabetes, and cancer [3–6]. Associated with obesity is adipocyte hypertrophy and hyperplasia, the latter being the

study design, data collection and analysis, decision to publish, or preparation of the manuscript.

**Competing interests:** The authors have declared that no competing interests exist.

direct consequence of increased adipogenic stimulation. It was originally assumed that adipocyte number rarely changed post adolescence. However, it is now known that approximately 10% of the adult body's adipocytes are replaced annually, highlighting the importance of adipogenesis [7].

The most commonly studied *in vitro* model of adipogenesis is the murine-derived 3T3-L1 cell line, first isolated by Green and Kehinde in 1974 [8]. These cells can be directed to accumulate lipids and adopt an adipocyte-like phenotype [9]. Human mesenchymal stem cells (hMSCs) also differentiate into adipocytes, and represent another useful model of adipogenesis [10]. It should be noted however, that unlike 3T3-L1 cells, hMSCs do not require a mitotic clonal expansion phase before adipogenesis is initiated [10, 11]. Moreover, the differentiation of hMSCs into mature adipocytes occurs in two phases; a determination phase where hMSCs commit to adipogenesis and become pre-adipocytes, and a differentiation phase where pre-adipocytes, in a manner similar to 3T3-L1 cells, begin secreting adipocyte-specific proteins and accumulate lipids [11, 12].

Although adipogenesis follows a relatively discrete series of events, it remains strongly influenced by extracellular factors, principally the extracellular matrix (ECM). During adipogenic differentiation of the pre-adipocyte, fibronectin-rich ECM is converted to a looser adipocyte basement membrane, suggesting direct involvement of matrix metalloproteinases (MMPs), a family of enzymes that utilized catalytically active zinc(II) to hydrolyze and modulate almost every ECM component [13]. Following the discovery of MMPs, numerous synthetic inhibitors have been created that incorporate a variety of zinc-binding groups (ZBGs) including hydroxamates, carboxylates, and phosphinyls [14–15]. The most potent matrix metalloproteinase inhibitors (MMPi) utilize hydroxamates, which coordinate  $Zn^{2+}$  in a bidentate fashion [15, 16]. However, the affinity for  $Zn^{2+}$  displayed by hydroxamate ZBGs tends to overwhelm proteinase specificity and lead to target promiscuity. As a result, our group focused on developing MMPi that contain the less implemented mercaptan ZBG [17–26]. The current YHJ series of MMPi incorporates a mercaptosulfonamide attached to a diphenyl ether to increase selectivity between MMPs based on S1' pocket depth [25–28]. Our latest inhibitors also display potencies similar to hydroxamate MMPi for a number of MMPs [26]. Consequently, we sought to determine if one of our most promising inhibitors, YHJ-7-52, could affect the adipogenic differentiation of hMSCs.

## Materials and methods

### Materials

The mercaptosulfide matrix metalloproteinase (MMP) inhibitor, YHJ-7-52, and its structural control, YHJ-7-82, were designed and synthesized by Drs. Martin A. Schwartz and Yonghao Jin as described [24, 26]. GM6001 was synthesized by Dr. Yonghao Jin. Troglitazone and T0070907 were purchased from Cayman Chemical Co. (Ann Arbor, MI). The adult human mesenchymal stem cell (hMSC) line was obtained from the Tulane University Center of Gene Therapy (New Orleans, LA). Human fibroblast collagenase (MMP-1) and gelatinase A (MMP-2) were provided by Dr. L. Jack Windsor (Indiana University, Indianapolis, IN) [27], recombinant human matrilysin-1 (MMP-7) was provided by Dr. Harold E. Van Wart (Syntex, Palo Alto, CA) [28], human neutrophil gelatinase B was purified from human blood by Dr. Qing-Xiang Sang as described previously [29], and human recombinant membrane-type 1 matrix metalloproteinase (MT1-MMP, MMP-14) was provided by Dr. Harald Tscheche (Bielefeld University, Bielefeld, Germany) [22–23]. All other commonly used reagents and materials were obtained from either VWR (Radnor, PA) or Sigma Aldrich (St. Louis, MO) unless otherwise specified.

## Enzyme inhibition assay

Enzymatic assays to characterize inhibitor potency were performed as previously described [22, 30]. Assays were performed at 25°C in 50 mM 4-(2-hydroxyethyl)-1-piperazineethanesulfonic acid (HEPES) buffer at pH 7.5 with 10 mM CaCl<sub>2</sub>, 200 mM NaCl, 0.01% (w/v) Brij-35, and 5 μM tris(2-carboxyethyl)-1-piperazineethanesulfonic acid (TCEP). The fluorogenic substrate Mca-PLGLDpa-AR-NH<sub>2</sub> (M-1895, Bachem, Torrance, CA) was used at a concentration of 1 μM as the substrate to measure inhibition constants. Briefly, 10 μL of inhibitor solution or control (100% DMSO), 176 μL of assay buffer, and 10 μL of enzyme solution were mixed and incubated for 30 min prior to initiation of the assay, which was accomplished by adding 4 μL of substrate solution, 5% final concentration DMSO. The release of product was monitored by fluorescence ( $\lambda_{\text{ex}} = 328 \text{ nm}$ ,  $\lambda_{\text{em}} = 393 \text{ nm}$ ) with a PerkinElmer luminescence spectrophotometer LS50B (FL WinLab v3.0) connected to a temperature-controlled water bath. Inhibitor potency was determined *via* comparison of relative rates ( $v_i/v_o$ ).

## Mesenchymal stem cell culture

Low passage human mesenchymal stem cells (hMSCs) were cultured in alpha-modified minimum essential medium ( $\alpha$ MEM) supplemented with an antibiotic cocktail composed of 10,000 IU penicillin and 10 mg/mL streptomycin, plus 200 mM L-glutamine, and 20% fetal bovine serum (FBS; GE Healthcare, Picataway, NJ). Prior to experimentation hMSCs were plated for 24 h of recovery and maintained at 37°C in a humidified environment containing 5% CO<sub>2</sub>. Cells were then seeded into appropriate culture ware, with media changed every 72 h until the desired confluence was reached.

## Cytotoxicity assay

Mercaptosulfonamide MMPIs were dissolved in 100% DMSO to generate 8 mM stock solutions and subsequently diluted with  $\alpha$ MEM, while maintaining the final DMSO concentration at 1.25% (v/v). Media supplemented with a panel of final inhibitor concentrations ranging from 0–100 μM were then added to 70–80% confluent hMSC cultures and incubated for 24 h. At the end of treatment, inhibitor-conditioned media was removed and cells were washed with phosphate buffered saline (PBS) (pH 7.4) prior to being trypsinized (0.25% Trypsin, GE Healthcare), pelleted, and resuspended in 1 mL of fresh  $\alpha$ MEM. Aliquots of the cell suspension for each condition were diluted 1:1 with 0.4% (w/v) Trypan Blue and counted with a hemocytometer. Relative cytotoxicity was determined by normalizing cell number for each condition against its respective control. A concentration was arbitrarily deemed cytotoxic if it produced a statistically significant reduction in cell number when compared to DMSO controls.

## Induction of adipogenesis

Human MSCs were seeded into 6-well plates at 1,000 cells/cm<sup>2</sup>. Upon reaching 70–80% confluence hMSCs were induced towards an adipogenic lineage by adding dexamethasone (0.5 μM), 3-isobutyl-1-methylxanthine (0.5 μM), and indomethacin (50 μM) to the culture medium [31]. Tested compounds were dissolved in DMSO and added to treatment wells during differentiation to a final total concentration of 10 μM with DMSO concentrations remaining constant (0.125% or 0.25% v/v) between conditions. Wells treated with appropriate concentrations of DMSO alone served as controls. Media and treatments were refreshed every 72 h for 21 days.

## Cell staining and quantification of lipid accumulation

After 21 days of differentiation, hMSCs were washed with PBS and fixed with neutral buffered formalin for 1 h. Cells were then stained with 0.3% (w/v) Oil Red-O in 3:2 100% isopropyl alcohol to PBS for 20 min, washed with PBS, stained with 5  $\mu$ g/mL Hoechst 33342 for 5 min, then washed again. Cultures were later imaged with an epifluorescence capable Nikon TE2000-E2 Eclipse microscope. Relative staining was determined with ImageJ (version 1.46c, National Institutes of Health, Bethesda, MD) by standardizing the area stained in each image to nuclei number prior to normalizing against DMSO treated controls.

## Quantitative real-time polymerase chain reaction (qPCR)

MMPI treated and untreated hMSCs were collected every 72 h over 21 days of differentiation. Total RNA from each time point was isolated using the E.Z.N.A. Total RNA Kit I (Omega Bio-Tek, Norcross, GA) and purified with the DNA-free RNA Kit (Zymo Research, Irvine, CA). RNA was resuspended in nuclease-free water, with concentrations determined *via* a Nanodrop UV-Vis Spectrophotometer (ThermoFisher Scientific, Waltham, MA). 500 ng of RNA was used for cDNA synthesis using qScript cDNA SuperMix (Quanta Bioscience, Gaithersburg, MD). 100 ng/ $\mu$ L cDNA was used as template for quantitative PCR on a 7500 Fast Real Time PCR system (Life Technologies, Carlsbad, CA) using PerfeCTa SYBR<sup>®</sup> Green SuperMix, Low Rox (Quanta Bioscience). Relative gene expression was determined via the  $2^{(-\Delta\Delta Ct)}$  method [32]. Expression levels of PPAR $\gamma$  (peroxisome-proliferator activated receptor gamma) were determined.  $\beta$ -Actin was used as an endogenous control. Primers were designed with Primer-BLAST (NCBI) and purchased from Integrated DNA Technologies (IDT, Coralville, IA). MMP-2: forward: 5' -CATCGCTCAGATCCGTGGTG-3' reverse: 5' -GCATCAATCTTTTCCG GGAGC-3'; MMP-14: forward: 5' -GGCTGCCTACCGACAAGATT-3' Reverse: 5' -GTACTC GCTATCCACTGCCC-3'; PPAR $\gamma$ : forward: 5' -CTTGCACTGGGGATGTCTCAT-3' reverse: 5' -AGGTCAGCGGACTCTGGATT-3';  $\beta$ -Actin: forward: 5' -AGTCCTGTGGCATCCACGAA CTA-3' reverse: 5' -ACTCCTGCTTGCTGATCCACATCT-3'.

## Statistical analysis

All cellular and qPCR experiments described above were performed with at least three independent replicates per data point and results are expressed as the mean  $\pm$  standard error. Kinetics results were repeated with three independent replicates and expressed as the mean  $\pm$  standard error. Statistical analyses were performed with the least significant difference correction for one-way analysis of variance (ANOVA) for multiple comparisons followed by Tukey contrast post-hoc analysis, with statistically significant values defined as  $P < 0.05$ .

## Results

### YHJ-7-52 is a potent MMP-2 and MMP-14 inhibitor

Fluorogenic substrate-based enzyme inhibition assays were performed to determine IC<sub>50</sub> values for the matrix metalloproteinase inhibitor (MMPI) YHJ-7-52. The potent broad-spectrum hydroxamate MMPI, GM6001, was used for comparison. The structural analog of YHJ-7-52, YHJ-7-82, was used as a negative control. YHJ-7-82 replaces the inhibitory thiol moiety with a non-inhibitory hydroxyl group. Compounds were evaluated for their potencies against a panel of MMPs relevant to adipogenesis [33]. Results are summarized in Table 1. YHJ-7-52 was highly potent for all deep and intermediate pocket MMPs, especially MMP-2 (gelatinase A) and MMP-14 (membrane-type 1 matrix metalloproteinase, MT1-MMP) where IC<sub>50</sub> values were less than 6 nM. GM6001 was highly potent against every MMP tested with IC<sub>50</sub> values

**Table 1. IC<sub>50</sub> values for the mercaptosulfonamide MMP inhibitor YHJ-7-52, its negative control compound YHJ-7-82, and GM6001.**

	IC <sub>50</sub> (nM)				
	MMP-1	MMP-2	MMP-7	MMP-9	MMP-14
YHJ-7-52	1200 ± 370	5.5 ± 4.2	2400 ± 720	87 ± 9	4.3 ± 0.7
YHJ-7-82	>200K	>100K	>200K	>200K	>200K
GM6001	0.4 ± 0.3	0.2 ± 0.1	2.0 ± 1.9	0.1 ± 0.1	0.5 ± 0.1

Enzyme inhibition kinetic assays were performed at 25°C in HEPES assay buffer containing 0.01% (w/v) Brij-35, and 5 μM TCEP. A fluorogenic substrate was used to measure MMP hydrolytic activity. The release of product was monitored by fluorescence. Inhibitor potency (IC<sub>50</sub> value) was determined *via* comparison of relative rates ( $v_i/v_0$ ). MMP—matrix metalloproteinase.

doi:10.1371/journal.pone.0172925.t001

equal to or less than 2 nM. The negative control compound YHJ-7-82 had almost undetectable inhibitory activity under the experimental conditions, indicating that the effectiveness of YHJ-7-52 is directly related to its zinc chelating group.

### YHJ-7-52 is effective in reducing lipid accumulation within cellular models of adipogenesis

To begin our investigation we examined if YHJ-7-52 and YHJ-7-82 displayed any cytotoxic effects. Human MSCs were treated with 0–100 μM of compound for 24 hours, stained with Trypan Blue, and live cells were counted. Fig 1A shows that YHJ-7-52 only produced a significant reduction in cell number at 100 μM, while its non-inhibitory analog, YHJ-7-82, showed minimal cytotoxicity across all tested concentrations. Based on the cytotoxicity results, a compound concentration of 10 μM was utilized for further examinations.

Next, we determined if YHJ-7-52 affected hMSC adipogenesis. Human MSCs were induced towards an adipogenic lineage in the presences of either YHJ-7-52, YHJ-7-82, or DMSO control. After 21 days differentiation was assessed by staining cells with Oil Red-O, and determining relative area of staining standardized to nuclei counts. Fig 1B and 1C show that treatment with YHJ-7-52 reduced lipid accumulation by approximately 36%, while YHJ-7-82 did not produce a significant response as anticipated.

### Gene expression levels of an adipogenic marker and two matrix metalloproteinases within human mesenchymal stem cells undergoing adipogenesis

Since image analysis only quantifies the extent of adipogenesis *via* measurements of lipid accumulation, quantitative real-time polymerase chain reaction (qPCR) was used to determine the effect of inhibitor treatment upon the transcriptional processes of hMSCs undergoing adipogenesis. For this experiment, the typical adipogenic marker, and a key regulator of adipogenesis, peroxisome-proliferator activated receptor gamma (PPARγ) was selected [34]. MMPs -2 and -14 (MT1-MMP) were selected because previous reports indicated they play principal roles in adipogenesis [33, 35].

Human mesenchymal stem cells (hMSCs) were induced to undergo adipogenic differentiation in the presence of YHJ-7-52 for 21 days with cells harvested every 72 h. Fig 2A shows treatment with YHJ-7-52 significantly suppressed PPARγ expression after day 9 of treatment when compared to DMSO controls. This indicates that YHJ-7-52 is influencing not only lipid accumulation but also differentiation. MMP-2 gene expression level was uniformly reduced after induction of adipogenesis by approximately 50%, while MMP-14 gene expression level remained relatively consistent (Fig 2B and 2C). These results indicate that YHJ-7-52 does not

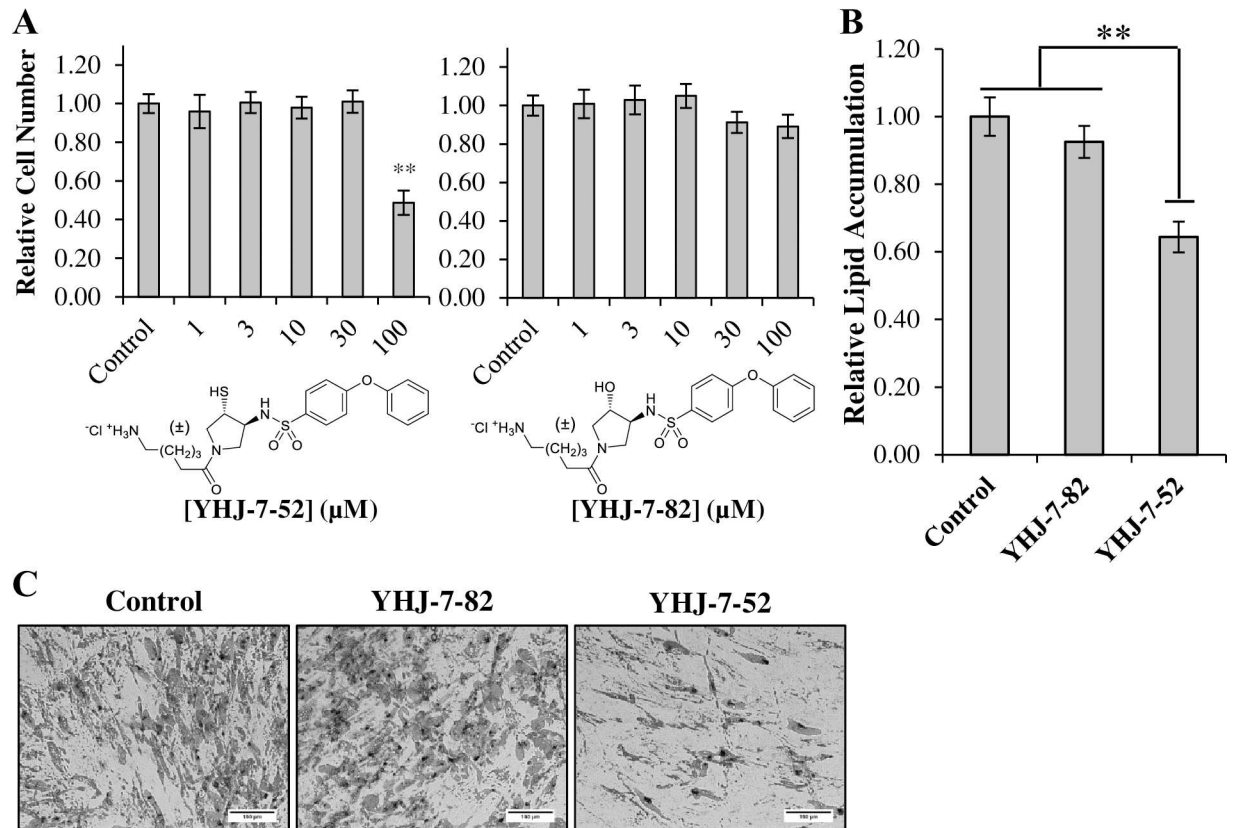


**Fig 1. Assessment of YHJ-7-52 biological activities in hMSC culture models.** (A) Human MSCs were incubated for 24 h with YHJ-7-52 and YHJ-7-82 at various concentrations (0–100 μM) and then counted. Human MSC were induced towards an adipogenic lineage in the presence of either 10 μM YHJ-7-52, 10 μM YHJ-7-82, or DMSO control. (B) Relative lipid accumulation as determined by imageJ. YHJ-7-52 reduced lipid accumulation by 36%. (C) Representative images of each condition. Results are displayed as mean ± standard error. Scale bar 150 μm. \*\*  $P < 0.05$

doi:10.1371/journal.pone.0172925.g001

affect MMP-2 and MMP-14 gene expression levels. For unknown reasons, on Day 21 upon the maturation of the adipocytes, the gene expression levels of MMP-2 and MMP-14 are significantly higher in the presence of YHJ-7-52 compared to the negative control.

### MMP inhibition reduces lipid accumulation in the presence of a peroxisome proliferator activated receptor gamma antagonist or agonist

Our results indicate that MMPI treatment reduces the adipogenic differentiation of hMSCs. Consequently, we wanted to determine if these compound could also produce effects in the presence of PPARγ modulators. To begin this investigation we assessed the extent to which the PPARγ agonist Troglitazone and antagonist T0070907 affect hMSC differentiation. We also included GM6001 as a positive control. Since T0070907 has an apparent IC<sub>50</sub> of ~1 nM [36], which is comparable to that of GM6001 and YHJ-7-52 for various MMPs, the final concentration used for these studies remained at 10 μM. Human MSCs were induced toward an adipogenic lineage for 21 days in the presence of either YHJ-7-52, YHJ-7-82, GM6001, T0070907, or Troglitazone. Treatment with T0070907 reduced lipid accumulation by 20%, similarly to that of YHJ-7-52 and GM6001, while Troglitazone increased lipid accumulation by approximately 80% (Fig 3).

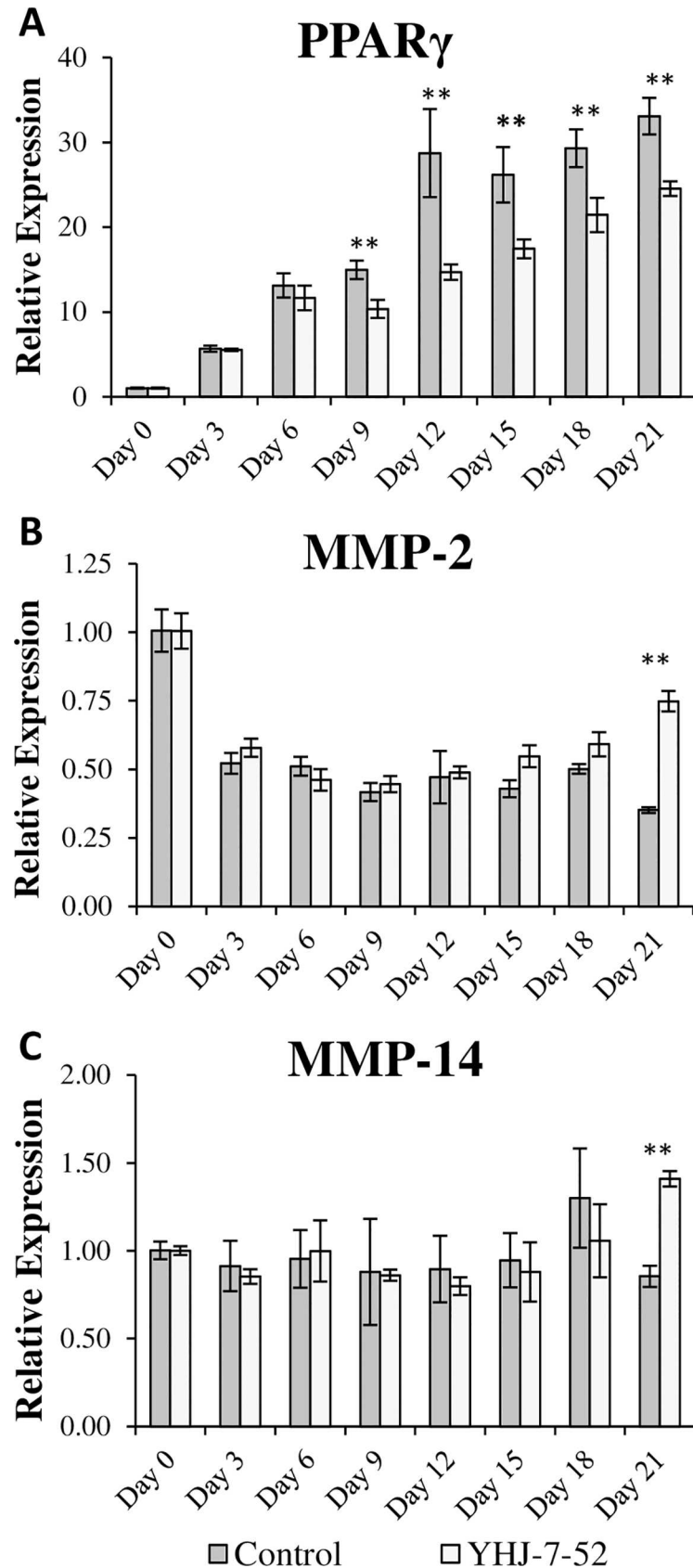


**Fig 2. Quantitative real-time PCR to measure gene expression levels of select adipogenic markers and MMPs in hMSCs induced toward an adipogenic lineage.** Human MSCs were treated with either YHJ-7-52 (10  $\mu$ M) or DMSO control. Expression of (A) PPAR $\gamma$ , (B) MMP-2, and (C) MMP-14 over time. Results are displayed as mean  $\pm$  standard error. \*\*  $P < 0.05$

doi:10.1371/journal.pone.0172925.g002

We next determined if co-treatment with MMPIs could reverse the increases of lipid accumulation simulated by Troglitazone. Fig 4 shows that while all treatment conditions displayed substantially more lipid accumulation than untreated controls, the addition of YHJ-7-52 and GM6001 significantly reduced the ability of Troglitazone to increase lipid accumulation (22% and 25% reduction respectively).

Finally, since MMPIs and T0070907 operated upon different targets, the ability of T0070907 to work synergistically with an MMPI when reducing adipogenesis was investigated (Fig 5A). When treated simultaneously with T0070907, both YHJ-7-52 and GM6001 further reduced lipid accumulation by ~20%. YHJ-7-82 did not provide any additional reductions consistent with previous results. Additionally, while treatment with T0070907 reduced relative cell number by approximately 30%, co-treatment with YHJ-7-52 did not result in further cell number reductions (Fig 5B).

## Discussion

### YHJ-7-52 affects adipogenesis possibly through the modulation of PPAR $\gamma$ mRNA expression

It was established early on that adipogenesis is highly influenced by the mechanical stresses imposed by extracellular matrices [8, 37–40]. Modulation of the ECM during adipogenesis is

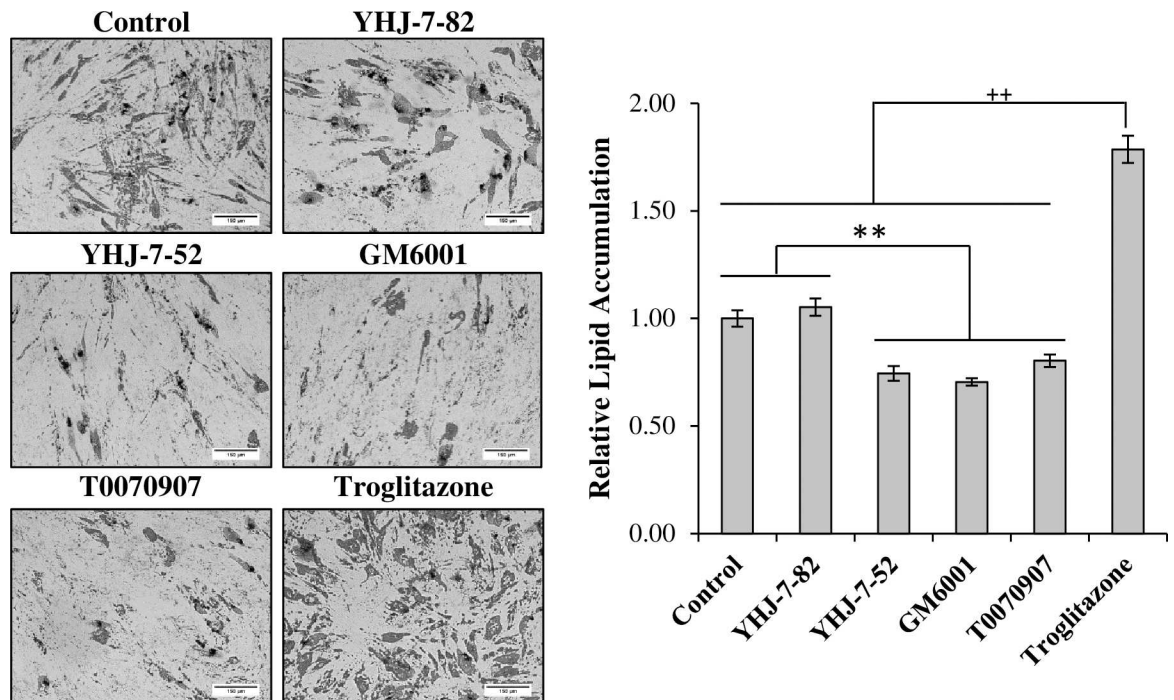


**Fig 3. Comparison of the effect of MMPIs and PPAR $\gamma$  modulators on adipogenesis.** Human MSCs undergoing adipogenic differentiation were cultured in the presence of either YHJ-7-82, YHJ-7-52, GM6001, T0070907, Troglitazone, or DMSO control. Final concentration of all compounds used was 10  $\mu$ M. Left, representative images detailing Oil Red-O staining. Right, imageJ analysis results. Results are displayed as mean  $\pm$  standard error. Scale bar 150  $\mu$ m. \*\*  $P < 0.05$ , ++  $P < 0.05$ .

doi:10.1371/journal.pone.0172925.g003

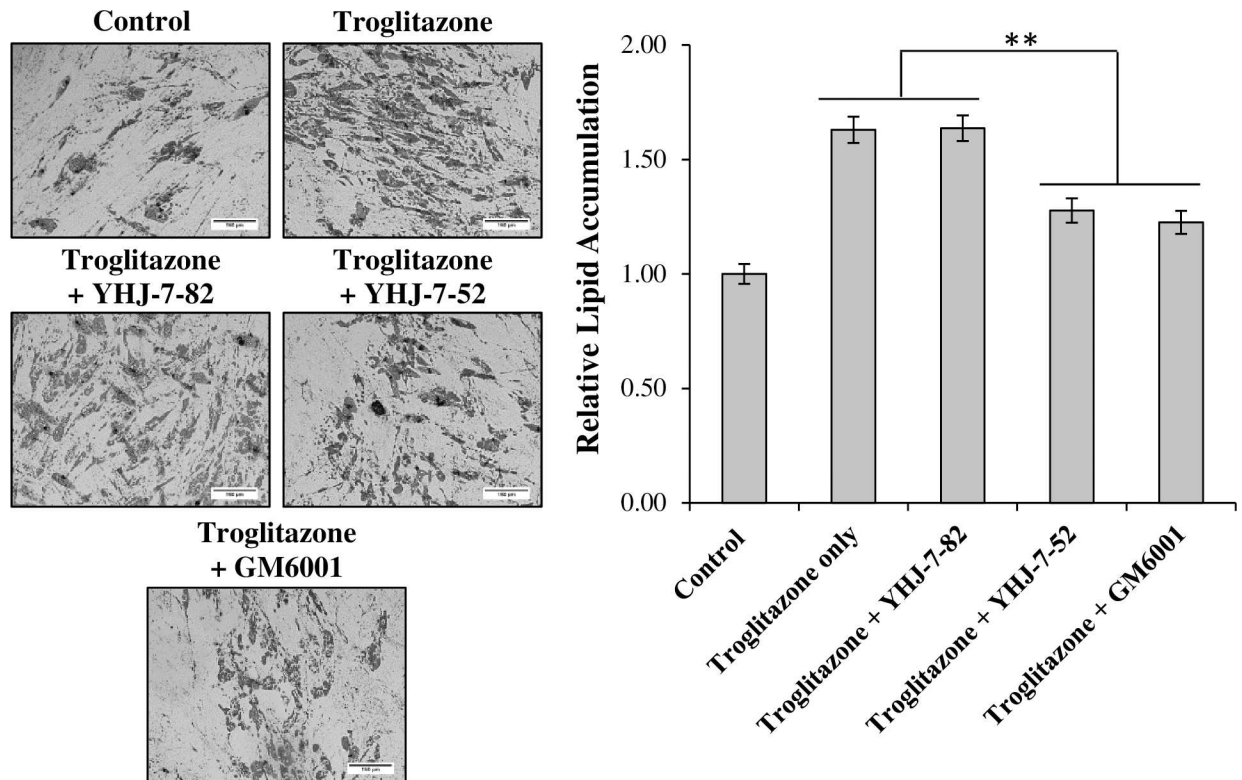


**Fig 4. Co-treatment of differentiating hMSCs with Troglitazone and MMPi.** Cells undergoing differentiation in the presence of 10  $\mu$ M Troglitazone were co-treated with either 10  $\mu$ M YHJ-7-82, YHJ-7-52, or GM6001. DMSO vehicle was maintained consistent between treatments and used as control. Results are displayed as mean  $\pm$  standard error. Scale bar 150  $\mu$ m. \*\*  $P < 0.05$ .

doi:10.1371/journal.pone.0172925.g004

suggested to influence cytoskeletal organization, which in turn can affect adipogenic signaling cascades, since the cytoskeleton provides a direct connection between the ECM and nuclear matrix [39, 41–48]. Furthermore, mechanical stress has been shown to affect the expression of PPAR $\gamma$  within stem cells undergoing adipogenesis [49]. Since, the primary means by which cells regulate ECM stiffness and composition is through the activity of MMPs, it was expected that YHJ-7-52 would affect PPAR $\gamma$  expression. Our qPCR results showed that YHJ-7-52 did indeed reduced PPAR $\gamma$  mRNA expression levels after days 9 of culture. However, complete suppression of PPAR $\gamma$  mRNA expression was not observed. Together with that fact that we observed a relatively similar reduction in lipid accumulation, it would indicate that MMPI treatment does not completely abolish adipogenic commitment within hMSCs, but it can influence the extent of differentiation.

### YHJ-7-52 and GM6001 display similar effects upon adipogenesis

During our earlier investigations with the YHJ series of thiol MMP inhibitors, we showed that while potent, they displayed lower levels of stability than hydroxamate compounds under standard enzyme inhibition assay conditions [26]. Despite having lower stability than the hydroxamate MMPI GM6001, YHJ-7-52 reduced lipid accumulation by similar amounts (Fig 3). One possibility is that the concentration used (10  $\mu$ M) is high enough to sustain the inhibitory activity for long enough periods of time to exert an influence. In addition, fetal bovine serum, which hMSCs require a greater percentage of, is composed of numerous factors including MMPs [50], thus a second possibility is that MMPs in the culture media, especially from fetal

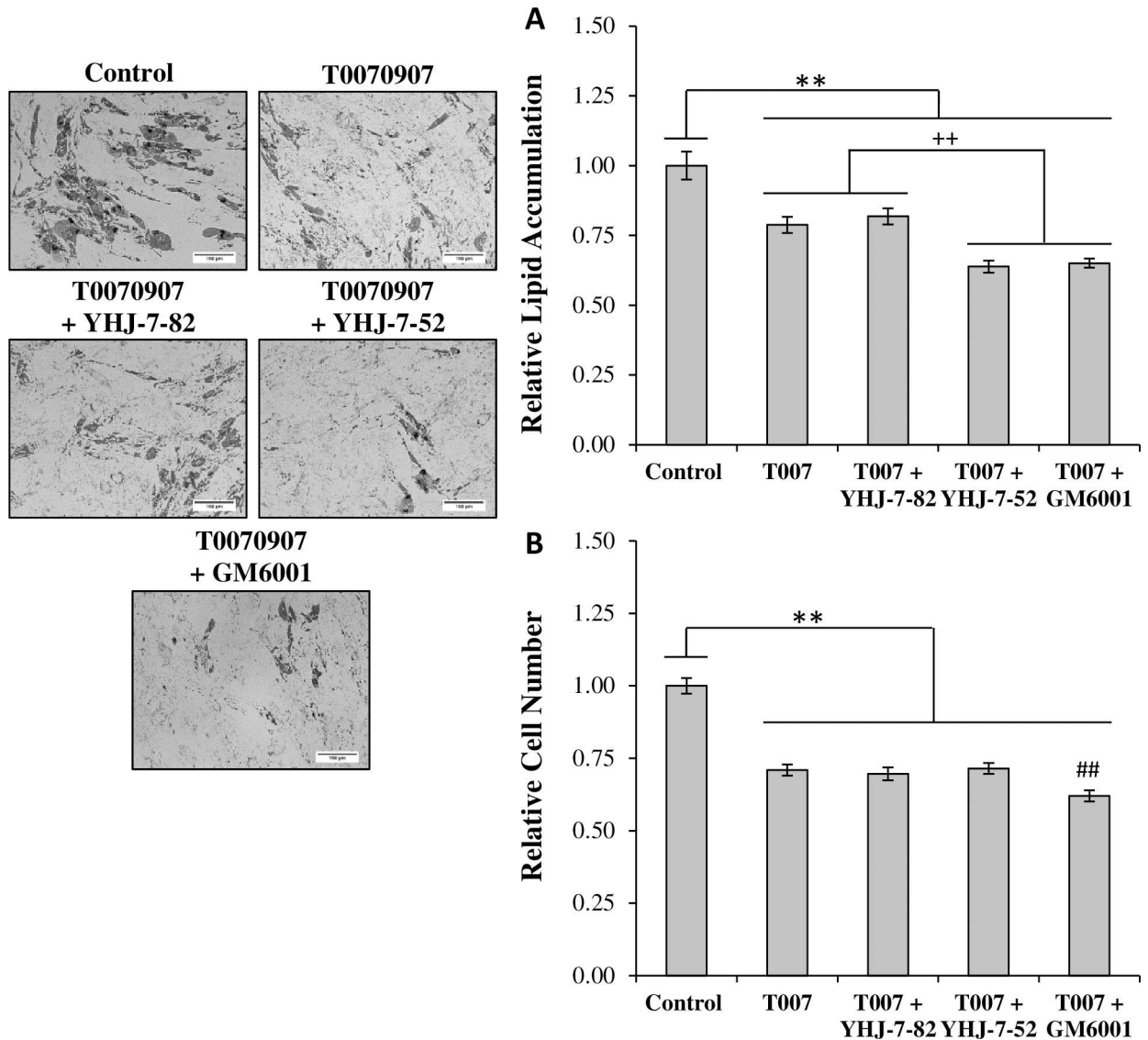


**Fig 5. Co-treatment of differentiating hMSCs with T0070907 and MMPi.** (A) Cells undergoing differentiation in the presence of 10  $\mu$ M T0070907 were co-treated with either 10  $\mu$ M YHJ-7-82, YHJ-7-52, or GM6001. DMSO vehicle was maintained consistent between treatments and used as control. (B) Relative cell number was determined via nuclei counts. Results are displayed as mean  $\pm$  standard error. Scale bar 150  $\mu$ m. \*\*  $P < 0.05$ , ++  $P < 0.05$ , ##  $P < 0.05$  compared to T0070907.

doi:10.1371/journal.pone.0172925.g005

bovine serum, may bind to MMP inhibitors and prevent thiol oxidation and MMPI inactivation as discussed in our previous publication [26].

### MMP inhibition can still reduce lipid accumulation in the presence of a peroxisome proliferator activated receptor gamma (PPAR $\gamma$ ) antagonist or agonist

Almost all previous studies investigating how MMPs affect obesity utilize either animal models or secondary metabolic markers in humans [33, 51–53]. However, numerous other factors can contribute to the outcome of these studies, such as angiogenesis [54] and macrophage activity [55]. As such, we decided to investigate the effects MMP inhibition had on overstimulation of

hMSC adipogenesis with the PPAR $\gamma$  agonist Troglitazone. We observed that both YHJ-7-52 and GM6001 reduced Troglitazone-induced lipid accumulation both by approximately 25% (Fig 4). While future studies will need to investigate the effects of YHJ MMPI treatment on whole human fat tissues, our results indicate that MMP inhibition can, to an extent, reduce the effects of PPAR $\gamma$  overstimulation during adipogenic differentiation and suggest that these MMPIs could be used as molecular tools for adipogenesis and obesity treatment research.

Finally, co-treatment experiments were performed using a MMPI and a PPAR $\gamma$  antagonist T0070907 to determine if these compounds could work together in reducing lipid accumulation. We observed that YHJ-7-52 and T0070907 co-treatment produced an additive reduction in lipid accumulation, while no additional reduction in cell number was observed. This, implies that observed cell number reductions were due to T0070907. T0070907 is reported to be minimally cytotoxic up to 50  $\mu$ M [56] and treatments up to 20  $\mu$ M have reduced proliferation of MDA-MB-231 and MCF-7 breast cancer cells without induction of apoptosis [57]. As a result, it is likely the observed reductions in cell number from these experiments stem from T0070907 reducing proliferation, not apoptosis. Thus, it would appear that MMPIs can work in combination with other modulators of adipogenesis without substantially affecting cell number, an important consideration in light of the physiological significance of adipose tissue.

## Conclusions

Our results show that the novel MMPI, YHJ-7-52, is an effective regulator of hMSC adipogenesis. Moreover, our inhibitor reduced PPAR $\gamma$  mRNA expression, attenuating adipogenesis in hMSCs. MMP inhibition was also able to suppress lipid accumulation in adipocytes co-treated with either Troglitazone, an efficacious agonist of PPAR $\gamma$ , or with T0070907, a potent antagonist of PPAR $\gamma$ . Therefore, MMP inhibition provides a potential avenue for adipogenesis and obesity treatment research.

## Acknowledgments

The authors would like to acknowledge the Tulane University Center of Gene Therapy (New Orleans, LA) for provision of the hMSC line.

## Author Contributions

**Conceptualization:** QXAS DBB.

**Data curation:** DBB MDR YHJ.

**Formal analysis:** DBB MDR YHJ QXAS.

**Funding acquisition:** QXAS MAS.

**Investigation:** DBB MDR YHJ TJL DARZ.

**Methodology:** DBB MDR YHJ.

**Project administration:** QXAS.

**Resources:** QXAS MAS.

**Supervision:** QXAS.

**Validation:** DBB YHJ MDR TJL DARZ.

**Visualization:** DBB YHJ MDR.

**Writing – original draft:** DBB.

**Writing – review & editing:** MDR YHJ MAS DARZ QXAS.

## References

1. Finkelstein E, Brown D, Wrage L, Allaire B, Hoerger J. Individual and aggregate years-of-life-lost associated with overweight and obesity. *Obesity*. 2010; 18:333–9. doi: [10.1038/oby.2009.253](https://doi.org/10.1038/oby.2009.253) PMID: [19680230](https://pubmed.ncbi.nlm.nih.gov/19680230/)
2. Mozaffarian D, Benjamin E, Go A, Arnett D, Blaha M, Cushman M, et al. Heart disease and stroke statistics—2015 update: a report from the American Heart Association. *Circulation*. 2015; 131:e29–e322. doi: [10.1161/CIR.000000000000152](https://doi.org/10.1161/CIR.000000000000152) PMID: [25520374](https://pubmed.ncbi.nlm.nih.gov/25520374/)
3. Hu F, Manson J, Stampfer M, Colditz G, Liu S, Solomon C, et al. Diet, lifestyle, and the risk of type 2 diabetes mellitus in women. *N Engl J Med*. 2001; 345: 790–797. doi: [10.1056/NEJMoa010492](https://doi.org/10.1056/NEJMoa010492) PMID: [11556298](https://pubmed.ncbi.nlm.nih.gov/11556298/)
4. Wilson P. W., D'Agostino R. B., Sullivan L., Parise H., Kannel W. B. Overweight and obesity as determinants of cardiovascular risk: The framingham experience. *Arch Intern Med*. 2002; 162:1867–1872. PMID: [12196085](https://pubmed.ncbi.nlm.nih.gov/12196085/)
5. Suk S, Sacco R, Boden-Albala B, Cheun J, Pittman J, Elkind M, et al. Northern Manhattan Stroke Study. Abdominal obesity and risk of ischemic stroke: The northern manhattan stroke study. *Stroke*. 2003; 34:1586–1592. doi: [10.1161/01.STR.0000075294.98582.2F](https://doi.org/10.1161/01.STR.0000075294.98582.2F) PMID: [12775882](https://pubmed.ncbi.nlm.nih.gov/12775882/)
6. De Pergola G, Silvestris F. Obesity as a major risk factor for cancer. *J Obes*. 2013; 2013:291546. doi: [10.1155/2013/291546](https://doi.org/10.1155/2013/291546) PMID: [24073332](https://pubmed.ncbi.nlm.nih.gov/24073332/)
7. Spalding K, Arner E, Westermark P, Bernard S, Buchholz B, Bergmann O, et al. Dynamics of fat cell turnover in humans. *Nature*. 2008; 453:783–787. doi: [10.1038/nature06902](https://doi.org/10.1038/nature06902) PMID: [18454136](https://pubmed.ncbi.nlm.nih.gov/18454136/)
8. Green H, Kehinde O. Sublines of mouse 3T3 cells that accumulate lipid. *Cell*. 1974; 1:113–116.
9. Green H, Kehinde O. An established preadipose cell line and its differentiation in culture. II. factors affecting the adipose conversion. *Cell*. 1975; 5:19–27. PMID: [165899](https://pubmed.ncbi.nlm.nih.gov/165899/)
10. Janderova L, McNeil M, Murrell A, Mynatt R, Smith S. Human mesenchymal stem cells as an in vitro model for human adipogenesis. *Obes Res*. 2003; 11:65–74. doi: [10.1038/oby.2003.11](https://doi.org/10.1038/oby.2003.11) PMID: [12529487](https://pubmed.ncbi.nlm.nih.gov/12529487/)
11. Muruganandan S, Roman A, Sinal C. Adipocyte differentiation of bone marrow-derived mesenchymal stem cells: cross talk with the osteoblastogenic program. *Cell Mol Life Sci*. 2009;66236–253.
12. Rosen E, MacDougald O. Adipocyte differentiation from the inside out. *Nat. Rev Mol Cell Biol*. 2006; 7:885–896. doi: [10.1038/nrm2066](https://doi.org/10.1038/nrm2066) PMID: [17139329](https://pubmed.ncbi.nlm.nih.gov/17139329/)
13. Lilla J, Stickens D, Werb Z. Metalloproteinases and adipogenesis: A weighty subject. *Am J Pathol*. 2002; 160:1551–1554. doi: [10.1016/S0002-9440\(10\)61100-5](https://doi.org/10.1016/S0002-9440(10)61100-5) PMID: [12000705](https://pubmed.ncbi.nlm.nih.gov/12000705/)
14. Visse R, Nagase H. Matrix metalloproteinases and tissue inhibitors of metalloproteinases: Structure, function, and biochemistry. *Circ Res*. 2003; 92:827–839. doi: [10.1161/01.RES.0000070112.80711.3D](https://doi.org/10.1161/01.RES.0000070112.80711.3D) PMID: [12730128](https://pubmed.ncbi.nlm.nih.gov/12730128/)
15. Whittaker M, Floyd C, Brown P, Gearing A. Design and therapeutic application of matrix metalloproteinase inhibitors. *Chem Rev*. 1999; 99:2735–2776. PMID: [11749499](https://pubmed.ncbi.nlm.nih.gov/11749499/)
16. Supuran C, Scozzafava A. Matrix Metalloproteinases (MMPs). In *Proteinase and Peptidase Inhibition: Recent Potential Targets for Drug Development*, Smith H. J., Simons C., Eds., Taylor & Francis, London and New York, 2002; 35–67.
17. White C. Pharmacologic, pharmacokinetic, and therapeutic differences among ACE inhibitors. *Pharmacotherapy*. 1998; 18:588–599. PMID: [9620109](https://pubmed.ncbi.nlm.nih.gov/9620109/)
18. Schwartz M, Van Wart H. Mercaptosulfide metalloproteinase inhibitors. U.S. Patent 5455262. 1995.
19. Sang Q, Schwartz M, Li H, Chung L, Zhau E. Targeting matrix metalloproteinases in human prostate cancer. *Ann. N.Y. Acad. Sci*. 1999; 878:538–540 PMID: [10415766](https://pubmed.ncbi.nlm.nih.gov/10415766/)
20. Sang Q, Jia M, Schwartz M, Jaye M, Kleinman H, Ghaffari M, et al. New thiol and sulfodiimine metalloproteinase inhibitors and their effect on human microvascular endothelial cell growth. *Biochem Biophys Res Commun*. 2000; 274:780–786. doi: [10.1006/bbrc.2000.3212](https://doi.org/10.1006/bbrc.2000.3212) PMID: [10924354](https://pubmed.ncbi.nlm.nih.gov/10924354/)
21. Park H, Jin Y, Hurst D, Monroe C, Lee S, Schwartz M, et al. The intermediate S1' pocket of the endomethase/matrilysin-2 active site revealed by enzyme inhibition kinetic studies, protein sequence analyses, and homology modeling. *J Biol Chem*. 2003; 278:51646–51653. doi: [10.1074/jbc.M310109200](https://doi.org/10.1074/jbc.M310109200) PMID: [14532275](https://pubmed.ncbi.nlm.nih.gov/14532275/)

22. Hurst D, Schwartz M, Ghaffari M, Jin, Tschesche H, Fields G, et al. Catalytic- and ecto-domains of membrane type 1-matrix metalloproteinase have similar inhibition profiles but distinct endopeptidase activities. *Biochem J.* 2004; 377:775–779. doi: [10.1042/BJ20031067](https://doi.org/10.1042/BJ20031067) PMID: [14533979](https://pubmed.ncbi.nlm.nih.gov/14533979/)
23. Hurst D, Schwartz M, Jin Y, Ghaffari M, Kozarekar P, Cao J, et al. Inhibition of enzyme activity of and cell-mediated substrate cleavage by membrane type 1 matrix metalloproteinase by newly developed mercaptosulphide inhibitors. *Biochem J.* 2005; 392:527–536. doi: [10.1042/BJ20050545](https://doi.org/10.1042/BJ20050545) PMID: [16026329](https://pubmed.ncbi.nlm.nih.gov/16026329/)
24. Schwartz M, Jin Y, Sang Q. Substituted Heterocyclic Mercaptosulfonamide Metalloprotease Inhibitors. U.S. Patent 8404866. 2013.
25. Jin Y, Ghaffari M, Schwartz M. A practical synthesis of differentially-protected cis-1,2-cyclopentane-dithiols and cis-3,4-pyrrolidinedithiols. *Tetrahedron Lett.* 2002; 43:7319–7321.
26. Jin Y, Roycik M, Bosco D, Cao Q, Constantino M, Schwartz M, et al. Matrix metalloproteinase inhibitors based on the 3-mercaptopyrrolidine core. *J Med Chem.* 2013; 56:4357–4373. doi: [10.1021/jm400529f](https://doi.org/10.1021/jm400529f) PMID: [23631440](https://pubmed.ncbi.nlm.nih.gov/23631440/)
27. Sang Q, Bodden M, Windsor L. Activation of human progelatinase A by collagenase and matrilysin: activation of procollagenase by matrilysin. *J Protein Chem.* 1996; 15:243–53. PMID: [8804571](https://pubmed.ncbi.nlm.nih.gov/8804571/)
28. Netzel-Arnett S, Sang Q, Moore W, Navre M, Birkedal-Hansen H, Van Wart H. Comparative sequence specificities of human 72- and 92-kDa gelatinases (type IV collagenases) and PUMP (matrilysin). *Biochemistry.* 1993; 32:6427–6432. PMID: [8390857](https://pubmed.ncbi.nlm.nih.gov/8390857/)
29. Sang Q, Birkedal-Hansen H, Van Wart H. Proteolytic and non-proteolytic activation of human neutrophil progelatinase B *Biochim Biophys Acta.* 1995; 1251:99–108. PMID: [7669817](https://pubmed.ncbi.nlm.nih.gov/7669817/)
30. Park H, Turk B, Gerkema F, Cantley L, Sang Q. Peptide substrate specificities and protein cleavage sites of human endometase/matrilysin-2/matrix metalloproteinase-26. *J Biol Chem.* 2002; 277:35168–35175. doi: [10.1074/jbc.M205071200](https://doi.org/10.1074/jbc.M205071200) PMID: [12119297](https://pubmed.ncbi.nlm.nih.gov/12119297/)
31. Sekiya I, Larson B, Vuoristo J, Chi J, Prockop D. Adipogenic differentiation of human adult stem cells from bone marrow stroma (MSCs). *J Bone Miner Res.* 2004; 19:256–264. doi: [10.1359/JBMR.0301220](https://doi.org/10.1359/JBMR.0301220) PMID: [14969395](https://pubmed.ncbi.nlm.nih.gov/14969395/)
32. Livak K, Schmittgen T. Analyzing of relative gene expression data using real-time quantitative PCR and the 2- $\Delta\Delta$ Ct method. *Methods.* 2001; 25:402–408. doi: [10.1006/meth.2001.1262](https://doi.org/10.1006/meth.2001.1262) PMID: [11846609](https://pubmed.ncbi.nlm.nih.gov/11846609/)
33. Chavey C, Mari B, Monthouel M, Bonnafous S, Anglard P, Van Obberghen E, et al. Matrix metalloproteinases are differentially expressed in adipose tissue during obesity and modulate adipocyte differentiation. *J Biol Chem.* 2003; 278:11888–11896. doi: [10.1074/jbc.M209196200](https://doi.org/10.1074/jbc.M209196200) PMID: [12529376](https://pubmed.ncbi.nlm.nih.gov/12529376/)
34. Nakamura T, Shiojima S, Hirai Y, Iwama T, Tsuruzoe N, Hirasawa A, et al. Temporal gene expression changes during adipogenesis in human mesenchymal stem cells. *Biochem Biophys Res Commun.* 2003; 303:306–312. PMID: [12646203](https://pubmed.ncbi.nlm.nih.gov/12646203/)
35. Chun T, Hotary K, Sabeh F, Saltiel A, Allen E, Weiss S. A pericellular collagenase directs the 3-dimensional development of white adipose tissue. *Cell.* 2006; 125:577–591. doi: [10.1016/j.cell.2006.02.050](https://doi.org/10.1016/j.cell.2006.02.050) PMID: [16678100](https://pubmed.ncbi.nlm.nih.gov/16678100/)
36. Lee G, Elwood F, McNally J, Weiszmann J, Lindstrom M, Amaral K, et al. T0070907, a selective ligand for peroxisome proliferator-activated receptor gamma, functions as an antagonist of biochemical and cellular activities. *J Biol Chem.* 2002; 277:19649–19657. doi: [10.1074/jbc.M200743200](https://doi.org/10.1074/jbc.M200743200) PMID: [11877444](https://pubmed.ncbi.nlm.nih.gov/11877444/)
37. Spiegelman B, Ginty C. Fibronectin modulation of cell shape and lipogenic gene expression in 3T3-adipocytes. *Cell.* 1983; 35:657–666. PMID: [6686086](https://pubmed.ncbi.nlm.nih.gov/6686086/)
38. Gumbiner B. Cell adhesion: The molecular basis of tissue architecture and morphogenesis. *Cell.* 1996; 84:345–357. PMID: [8608588](https://pubmed.ncbi.nlm.nih.gov/8608588/)
39. McBeath R, Pirone D, Nelson C, Bhadriraju K, Chen C. Cell shape, cytoskeletal tension, and RhoA regulate stem cell lineage commitment. *Dev Cell.* 2004; 6:483–495. PMID: [15068789](https://pubmed.ncbi.nlm.nih.gov/15068789/)
40. Fukai F, Ohtaki M, Fujii N, Yajima H, Ishii T, Nishizawa Y, et al. Release of biological activities from quiescent fibronectin by a conformational change and limited proteolysis by matrix metalloproteinases. *Biochemistry.* 1995; 34:11453–11459. PMID: [7547873](https://pubmed.ncbi.nlm.nih.gov/7547873/)
41. Jones P, Schmidhauser C, Bissell M. Regulation of gene expression and cell function by extracellular matrix. *Crit Rev Eukaryot Gene Expr.* 1993; 3:137–54. PMID: [8324293](https://pubmed.ncbi.nlm.nih.gov/8324293/)
42. Smas C, Sul H. Control of adipocyte differentiation. *Biochem J.* 1995; 309:697–710. PMID: [7639681](https://pubmed.ncbi.nlm.nih.gov/7639681/)
43. Akimoto T, Ushida T, Miyaki S, Akaogi H, Tsuchiya K, Yan Z, et al. Mechanical stretch inhibits myoblast-to-adipocyte differentiation through wnt signaling. *Biochem Biophys Res Commun.* 2005; 329:381–385. doi: [10.1016/j.bbrc.2005.01.136](https://doi.org/10.1016/j.bbrc.2005.01.136) PMID: [15721317](https://pubmed.ncbi.nlm.nih.gov/15721317/)

44. Jakkaraju S, Zhe X, Pan D, Choudhury R, Schuger L. TlPs are tension-responsive proteins involved in myogenic versus adipogenic differentiation. *Dev. Cell.* 2005; 9:39–49. doi: [10.1016/j.devcel.2005.04.015](https://doi.org/10.1016/j.devcel.2005.04.015) PMID: [15992539](https://pubmed.ncbi.nlm.nih.gov/15992539/)
45. Sen B, Xie Z, Case N, Ma M, Rubin C, Rubin J. Mechanical strain inhibits adipogenesis in mesenchymal stem cells by stimulating a durable beta-catenin signal. *Endocrinology.* 2008; 149:6065–6075. doi: [10.1210/en.2008-0687](https://doi.org/10.1210/en.2008-0687) PMID: [18687779](https://pubmed.ncbi.nlm.nih.gov/18687779/)
46. Guilak F, Cohen D, Estes B, Gimble J, Liedtke W, Chen C. Control of stem cell fate by physical interactions with the extracellular matrix. *Cell Stem Cell.* 2009; 5:17–26. doi: [10.1016/j.stem.2009.06.016](https://doi.org/10.1016/j.stem.2009.06.016) PMID: [19570510](https://pubmed.ncbi.nlm.nih.gov/19570510/)
47. Noguchi M, Hosoda K, Fujikura J, Fujimoto M, Iwakura H, Tomita T, et al. Genetic and pharmacological inhibition of rho-associated kinase II enhances adipogenesis. *J Biol Chem.* 2007; 282:29574–29583. doi: [10.1074/jbc.M705972200](https://doi.org/10.1074/jbc.M705972200) PMID: [17681946](https://pubmed.ncbi.nlm.nih.gov/17681946/)
48. Dupont S, Morsut L, Aragona M, Enzo E, Giulitti S, Cordenonsi M, et al. Role of YAP/TAZ in mechano-transduction. *Nature.* 2011; 474:179–183. doi: [10.1038/nature10137](https://doi.org/10.1038/nature10137) PMID: [21654799](https://pubmed.ncbi.nlm.nih.gov/21654799/)
49. Poulos S, Dodson M, Culver M, Hausman G. The increasingly complex regulation of adipocyte differentiation. *Exp Biol Med (Maywood).* 2016; 241:449–56.
50. Hu X, Beeton C. Detection of functional matrix metalloproteinases by zymography. *J Vis Exp.* 2010; pii:2445.
51. Croissandeau G, Chretien M, Mbikay M. Involvement of matrix metalloproteinases in the adipose conversion of 3T3-L1 preadipocytes. *Biochem J.* 2002; 364:739–746. doi: [10.1042/BJ20011158](https://doi.org/10.1042/BJ20011158) PMID: [12049638](https://pubmed.ncbi.nlm.nih.gov/12049638/)
52. Derosa G, Ferrari I, D'Angelo A, Tinelli C, Salvadeo S, Ciccarelli L, et al. Matrix metalloproteinase-2 and -9 levels in obese patients. *Endothelium.* 2008; 15:219–224. doi: [10.1080/10623320802228815](https://doi.org/10.1080/10623320802228815) PMID: [18663625](https://pubmed.ncbi.nlm.nih.gov/18663625/)
53. Van Hul M, Lupu F, Dresselaers T, Buyse J, Lijnen H. Matrix metalloproteinase inhibition affects adipose tissue mass in obese mice. *Clin Exp Pharmacol Physiol.* 2012; 39:544–550. doi: [10.1111/j.1440-1681.2012.05714.x](https://doi.org/10.1111/j.1440-1681.2012.05714.x) PMID: [22519563](https://pubmed.ncbi.nlm.nih.gov/22519563/)
54. Cao Y. Adipose tissue angiogenesis as a therapeutic target for obesity and metabolic diseases. *Nat Rev Drug Discov.* 2010; 9:107–15. doi: [10.1038/nrd3055](https://doi.org/10.1038/nrd3055) PMID: [20118961](https://pubmed.ncbi.nlm.nih.gov/20118961/)
55. Wellen K, Hotamisligil G. Obesity-induced inflammatory changes in adipose tissue. *J Clin Invest.* 2003; 112:1785–1788. doi: [10.1172/JCI20514](https://doi.org/10.1172/JCI20514) PMID: [14679172](https://pubmed.ncbi.nlm.nih.gov/14679172/)
56. Pavlov T, Levchenko V, Karpushev A, Vandewalle A, Staruschenko A. Peroxisome proliferator-activated receptor gamma antagonists decrease Na<sup>+</sup> transport via the epithelial Na<sup>+</sup> channel. *Mol Pharmacol.* 2009; 76:1333–1340. doi: [10.1124/mol.109.056911](https://doi.org/10.1124/mol.109.056911) PMID: [19752200](https://pubmed.ncbi.nlm.nih.gov/19752200/)
57. Zaytseva Y, Wallis N, Southard R, Kilgore M. The PPARγ antagonist T0070907 suppresses breast cancer cell proliferation and motility via both PPARγ-dependent and -independent mechanisms. *Anticancer Res.* 2011; 31:813–823. PMID: [21498701](https://pubmed.ncbi.nlm.nih.gov/21498701/)